IEEE Access
Multidisciplinary | Rapid Review | Open Access Journal

Received January 29, 2021, accepted February 8, 2021, date of publication February 19, 2021, date of current version March 1, 2021.

Digital Object Identifier 10.1109/ACCESS.2021.3060588

Intrusive Passive Optical Tapping Device

ISMEL DOMÍNGUEZ[1,2], IGNACIO DEL VILLAR[1], (Member, IEEE), JORGE MONTOYA-CARDONA[3], OMAR FUENTES[4], NELSON D. GÓMEZ-CARDONA[3], JESUS M. CORRES[3], (Member, IEEE), AND IGNACIO R. MATIAS[2], (Senior Member, IEEE)

[1]Institute of Smart Cities, Public University of Navarre, 31006 Pamplona, Spain
[2]Department of Electrical, Electronic and Communications Engineering, Public University of Navarre, 31006 Pamplona, Spain
[3]Departamento de Electrónica y Telecomunicaciones, Instituto Tecnológico Metropolitano, Medellín 050013, Colombia
[4]Department of Telecommunications and Electronics, Pinar del Río University, Pinar del Río 20100, Cuba

Corresponding author: Ignacio R. Matias (natxo@unavarra.es)

This work was supported in part by the Spanish Agencia Estatal de Investigación (AEI) Research Funds under Grant PID2019-106231RB-I00 and Grant PID2019-106070RB-I00, in part by the Pre-Doctoral Research Grant of the Public University of Navarra, and in part by the InstitutoTecnologico Metropolitano under Project P20212.

ABSTRACT Passive optical tapping can be implemented by stacking multiple layers of polydimethylsiloxane (PDMS), which is used as planar waveguides for the transmission and capturing of light. Once the main waveguide is installed in the communications system, each additional stacked waveguide represents an optical sniffer where it is possible to intercept the data from an input optical fibre, allowing the information to also flow to the output fibre unnoticeably from the point of view of the transmitter. The waveguides can be stacked or removed, making it a dynamic device that overcomes the limitations of previous designs, and the optical sniffer shows fixed implementation. In addition, it is demonstrated that PDMS is a versatile material that permits the control of the coupling of light among the waveguides, depending on its properties, and the thickness of each waveguide is also critical for the performance of the device. Furthermore, the experimental results are supported with a theoretical analysis that permits better understanding of the performance of the device, whose use can be extended to other applications, such as a passive optical hub or a signal combiner/splitter.

INDEX TERMS Optical tapping, sniffer, optical communications interceptor, planar waveguides, photonic devices.

I. INTRODUCTION

Photonics play an increasingly important role in our world. Therefore, developing multipurpose platforms that allow the connection of the growing number of communication lines that are required in a society where all equipment must be interconnected is vital and is very much in line with the Internet of Things (IoT) or industry 4.0. Similarly, it is important to have hardware and software devices to intercept the flow of communication in a network so that it can identify unusual traffic, collect data for security analysis, detect peaks and valleys in the bandwidth used, and analyse performance, etc.

This requires a physical system that extracts the signal from the optical fibre without breaking (tapping) and a subsequent system consisting of an optoelectronic converter and software that analyses the extracted signal (network sniffer systems). In this sense, this work is focused on the physical device.

The associate editor coordinating the review of this manuscript and approving it for publication was Bo Pu.

There are a number of known methods for extracting or even injecting information into a fibre link. Basically, fibre tapping can be intrusive and non-intrusive. The former requires the fibre to be cut and reconnected into the tapping mechanism, while the later achieves tapping without cutting the fibre or causing any service disruption. Non-intrusive tapping is often related to malicious data hacks and is prosecuted by law. The more common technique is fibre bending, where a cable is stripped down to the fibre for bending. There exist commercial devices available that allow this tapping to be performed with losses of around 7 dB, such as the well-known Optical Clip-on Coupler [1]. Among the intrusive techniques, the most used is the technique based on optical splitting [1]–[4]. As with the rest of the intrusive techniques, this method causes some disruption on the line since the optical cable is split using a clip that cuts into the cable and attaches an optical splitter, which transmits light from the main input fibre to several output fibres. The insertion losses are important depending on the number of outputs of the splitter because

insertion losses are ruled by 10log(1/N), where N is the number of outputs [2]. In this case, as the signal is only briefly disrupted when the fibre is clipped, the tapping may remain undetected. In either case, intrusion can be detected using a simple optical time domain reflectometer (OTDR) [5].

The device presented in this work is an intrusive passive optical multiple tapping device based on polydimethylsiloxane (PDMS) waveguides that are located between an input and an output fibre. For this purpose, two concepts will be applied. The first concept, contrary to the conventional design, is the fabrication of waveguides with enough scattering to guarantee the transmission of light in all directions, and the second concept is the ability to dynamically stack or remove waveguides that are in direct contact with the optical fibre.

In view of these requirements, the key element of the device is the material. In this sense, the first condition that the material must satisfy is the ability to embed the optical fibre in order to avoid coupling or reflection problems. Materials that satisfy this condition are polymers. Indeed, research on artificial polymers has become of great importance in all fields of engineering, from bioengineering to electronics, which opens the path for customised designs. An artificial polymer that deserves special mention is PDMS, which has been increasingly applied in many research fields, such as protective coatings, analytical chemistry, microfluidics, the lab on a chip paradigm, and in flexible medical devices [6]–[10].

Regarding the second condition, the ability to stack different waveguides of PDMS is not a problem, and indeed the flexibility of this material permits better adhesion among the waveguides. Finally, the ability to scatter light is satisfied because PDMS is a material used for scattering control to the extent that it permits regulation of the transmission of light using methods such as the addition of TiO_2 particles [11] or glycerol [12]. This indicates that PDMS is versatile enough to be implemented in a dynamic optical tapping device.

II. EXPERIMENTAL SET-UPS

To obtain the experimental results, two different configurations were used. The first configuration aimed to analyse the insertion losses of the PDMS optical tapping device, which is described in Fig. 1a. The device consists of planar waveguides of PDMS that can be stacked or unstacked. The PDMS selected for the experiment was Sylgard 184 from Dow Corning. The samples were prepared by manually mixing the Sylgard 184A prepolymer with the Sylgard 184B curing agent in a 10:1 ratio. Two sets of samples were created, and in one set air was initially extracted with a vacuum pump. Then, the PDMS was cured in a hot plate with a magnetic stirrer (IKA RCT basic from Sigma-Aldrich) at a temperature of 100° C for 30 minutes.

After that, the first segment of PDMS was placed on a substrate with a refractive index lower than that of PDMS to avoid light losses towards the substrate. In this case, Teflon (polytetrafluoroethylene) was used, which typically has a refractive index of 1.35–1.38 [13]. PDMS has a higher refractive index of around 1.4 [14]. This main PDMS waveguide was connected at both ends to two multimode fibres (M72L01 of Thorlabs) with core and cladding diameters of 200 and 225 μm, respectively, and a numerical aperture of 0.39. The rest of the PDMS waveguides were connected at one end to a multimode fibre with the same characteristics as the multimode fibres of the main PDMS waveguide. As a result, one of the two fibres of the main PDMS waveguide was the input of the optical device, and the other fibre of the main PDMS waveguide and the fibres connected to the rest of the PDMS waveguides were the outputs. The input was connected to a light source (three different sources were tested: a RIFOCS 263A Laser Source at 635 nm, a RIFOCS 265A Laser Source at 1310 nm, and a RIFOCS 266A Laser Source at 1500 nm), whereas the outputs were connected to photodetectors (all were RIFOCS 555B Controller Power Meter).

Fig. 1b shows an experimental photograph where waveguide B is coupled to the main waveguide, waveguide A. Regarding the multimode fibres used in the experiment, they were manually coupled to the PDMS (no polishing of the end facet of the PDMS was needed). To achieve the best possible coupling of the fibre and PDMS, to transmit all the light to the material, and to be better seen with the naked eye, the coupling was done with the help of a 635 nm laser. One end of the fibre was connected to the laser light source (red), causing the other end of the fibre to reflect the laser. When the light at the tip of the fibre is coupled to the PDMS substrate, the reflected light disappears because it is transmitted through the PDMS. Therefore, we visually verified that the best possible coupling was achieved. This operation is repeated with the fibre that is at the other end of the PDMS substrate, once again guaranteeing good coupling. On the other hand, the correct alignment of the fibres with respect to the substrate also provides better transmission of light.

To extract part of the power or signal that is transmitted in this assembly, several PDMS tapping devices were built. The tip of a previously cut and polished multimode fibre is placed horizontally on a coverslip, and the fibre is fixed with the help of glue. One millilitre of PDMS is poured over this coverslip and rotated manually until the desired thickness of the PDMS film is attained. The PDMS is solidified by placing the coverslip on a hot plate at 100° C for 30 minutes. Then, the film is cut to dimensions of 1 cm × 1 cm, leaving the tip of the fibre right in the centre of the substrate.

At the other end of the aforementioned fibre, an FC/PC connector is placed, allowing the transmission of light to the measuring instruments. In this way, a device capable of extracting part of the optical signal that is transmitted through the PDMS substrate is obtained. By means of this procedure, two identical devices are obtained that demonstrate that the extraction of light or signal can be stackable, without affecting the original transmitted signal noticeably. Visualisation S1 also shows the coupling to the main waveguide and one of the waveguides stacked in the optical tapping device.

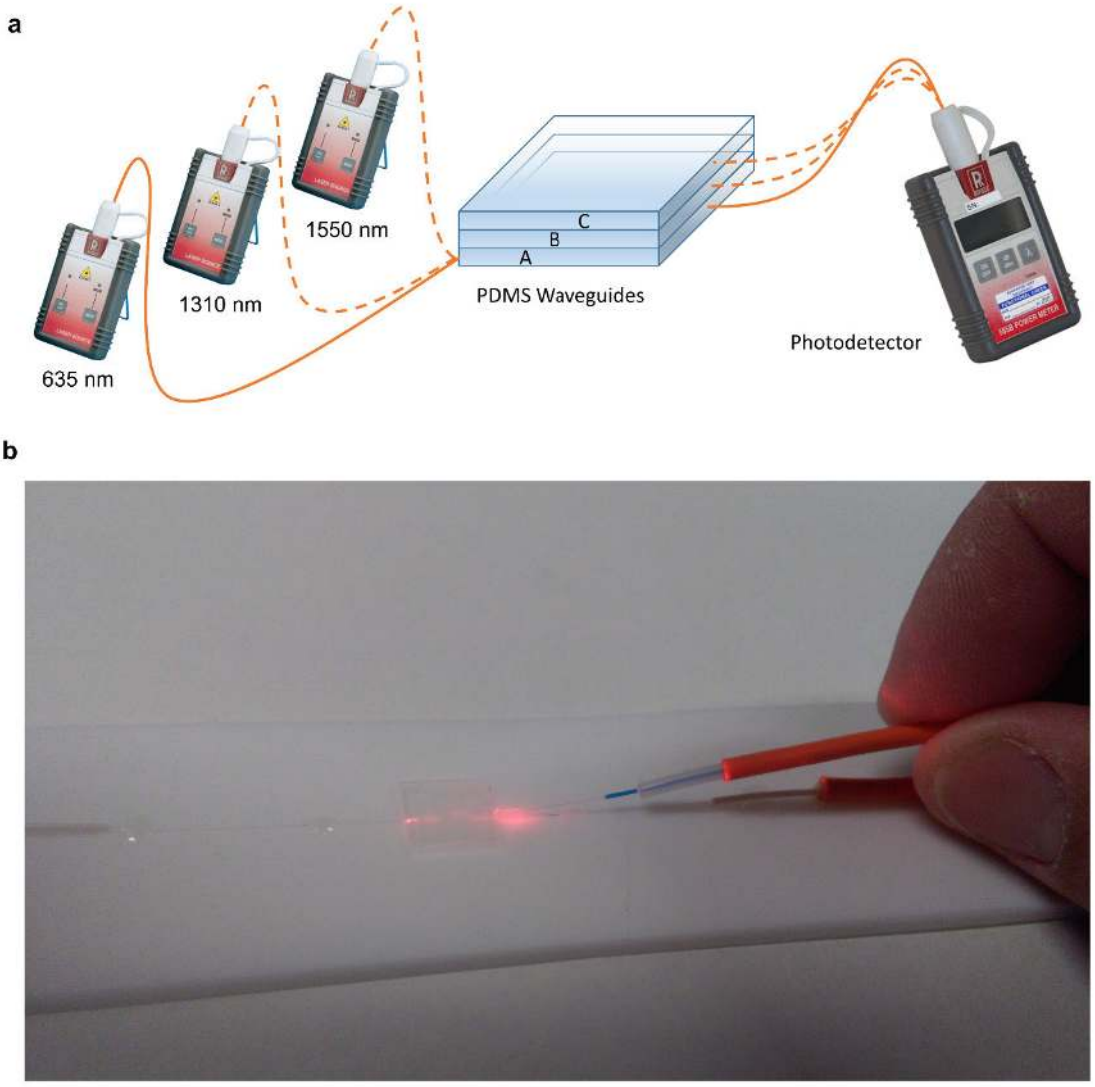

FIGURE 1. (a) Schematic setup for analysing the insertion losses in the optical tapping device. (b) Experimental placement of a tapping device on the main polydimethylsiloxane (PDMS) waveguide. Visualisation S1 also shows the coupling to the main waveguide and one of the waveguides stacked in the optical tapping device.

The second configuration (see Fig. 2) was used for analysing the quality of the communications. In this sense, various techniques can be used to analyse the behaviour of an optical communication, such as the bit error rate (BER), the signal to noise ratio (SNR) of the transmitted signal, or the attenuation. However, the best method is an analysis of the pulse waveforms that propagate along the platform, which makes it possible to observe their shapes, jitter, noise levels, signal strengths, etc. All this can be obtained with the eye diagram. For this purpose, an Agilent Technologies 81133A pulse generator was added to the system, with a module to generate patterns for the analysis of eye diagrams. This pulse generator modulates an HFBR-1414PTZ LED source, and the resulting signal is introduced in the input of the optical tapping device. The output of the optical tapping device is connected to the receiver, a silicon detector model AFBR-2418TZ (both the transmitter and the optical receiver belong to the AFBR-0549Z evaluation kit, with a bandwidth of 100 MHz). Finally, the optical receiver is connected to an Agilent Infiniium 54833A DSO model oscilloscope to compare the eye diagram of the input and the output signal.

For generation of the eye diagram, a pseudo random binary sequence (PRBS) with a pattern of 10^2-1 at 100 Mbps was used.

III. RESULTS

In the previous section, the design of the optical tapping device was presented along with the two configurations used in this work: one for the analysis of the insertion losses and the other for testing the performance of the device in optical communications. Now, the results obtained with both configurations will be presented along with a theoretical analysis, which allows us to better understand the experimental results obtained with the device.

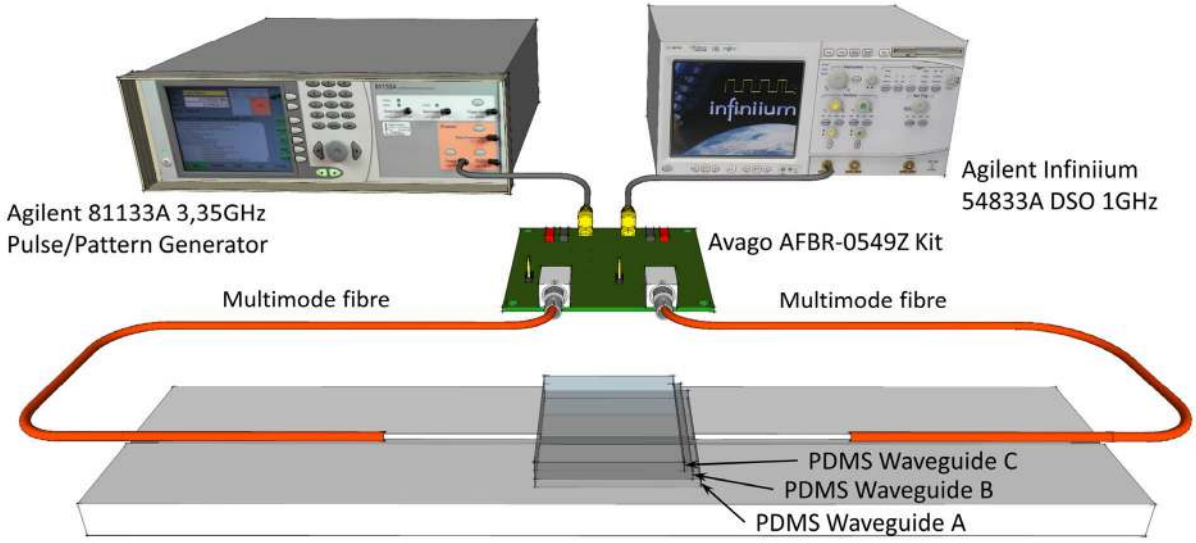

FIGURE 2. Setup for the analysis of the performance of the optical tapping device for communications.

A. EVALUATION OF THE INSERTION LOSSES

The first experiment was performed to determine the insertion losses of the optical tapping device represented in Fig. 1a, where three PDMS waveguides are stacked: waveguides A, B, and C. Light input is through the main waveguide, which is waveguide A.

Three devices were fabricated, all with a length of 1 cm and a width of 1 cm. The 1 cm width permitted to couple light from the optical source, whereas the 1 cm length was selected to meet two requirements: to reduce insertion losses with a device that was not too long and to not have a device that was too short in terms of handling.

Once the length was fixed, we had to consider that the beam, which was launched into the PDMS by the multimode fibres located at the input end, spreads during propagation. This spreading is governed by parameters such as the refractive index of the PDMS, the initial waist of the beam ($wo \approx 200\ \mu m$), and the numerical aperture (NA) of the multimode optical fibre ≈ 0.39. This is why the dimensions of the tapping devices must facilitate the coupling of light to the PDMS waveguide and next to the optical fibres located at the output end of the device.

The two properties that make the devices different are the thickness of the waveguides and the application (or not) of a vacuum process to remove air bubbles inside. For the first and second devices, devices D1 and D2, respectively, no vacuum process was applied to remove air bubbles inside, whereas the opposite was true for device D3. Regarding the waveguide thickness, PDMS waveguides of device D1 presented a thickness of 0.8 mm, whereas the waveguides in D2 and D3 presented a thickness of 0.5 mm. These two thickness values were selected to determine if the insertion loss obtained when one PDMS waveguide of thickness 0.8 mm was stacked on the main waveguide was in-between the values obtained by stacking one 0.5 mm PDMS waveguide or two 0.5 mm PDMS waveguides (1 mm).

TABLE 1. Insertion loss in the main waveguide (waveguide A) of device D1 (PDMS waveguides with a thickness of 0.8 mm and no vacuum applied to remove air bubbles).

Output	λ=635 nm	λ=1310 nm	λ=1550 nm
A before adhesion of tapping devices	–15.33 dB	–15.15 dB	–15.88 dB
A after adhesion of B	–17.24 dB	–17.11 dB	–18.15 dB
A after adhesion of C	–17.42 dB	–17.82 dB	–19.02 dB

TABLE 2. Insertion loss in the main waveguide (waveguide A) of device D2 (PDMS waveguides with a thickness of 0.5 and no vacuum applied to remove air bubbles).

Output	λ=635 nm	λ=1310 nm	λ=1550 nm
A before adhesion of tapping devices	–11.09 dB	–10.63 dB	–12.66 dB
A after adhesion of B	–14.21 dB	–13.95 dB	–15.77 dB
A after adhesion of C	–15.64 dB	–15.26 dB	17.21 dB

TABLE 3. Insertion loss in the main waveguide (waveguide A) of device D3 (PDMS waveguides with a thickness of 0.5 mm and vacuum applied to remove air bubbles).

Output	λ=635 nm	λ=1310 nm	λ=1550 nm
A before adhesion of tapping devices	–15.27 dB	–13.33 dB	–17.19 dB
A after adhesion of B	–16.01 dB	–13.84 dB	–17.20 dB
A after adhesion of C	–15.42 dB	–12.98 dB	–17.52 dB

Tables 1, 2, and 3 correspond to D1, D2, and D3, respectively. They show the insertion loss in the visible region and at the infrared standard telecommunication windows of the main waveguide (waveguide A) when several PDMS waveguides are progressively stacked on it.

Regarding D1, in Table 1 it can be observed that the insertion loss after the addition of two PDMS waveguides (waveguide B and waveguide C) increases by 2.09 dB at 635 nm, by 2.67 dB at 1310 nm, and by 3.2 dB at 1550 nm,

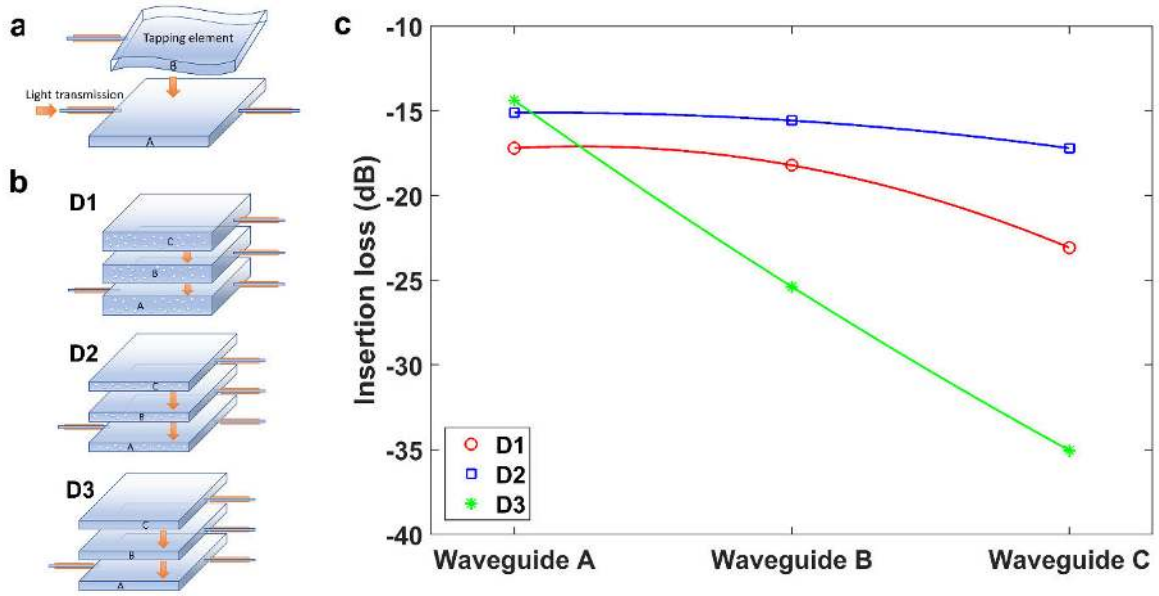

FIGURE 3. Insertion losses for waveguides A, B, and C in three optical tapping devices at 1310 nm: D1 (waveguides with a thickness of 0.8 mm and no vacuum applied to remove trapped air bubbles), D2 (waveguides with a thickness of 0.5 mm and no vacuum applied to remove trapped air bubbles), and D3 (waveguides with a thickness of 0.5 mm and vacuum applied to remove trapped air bubbles).

observing an increase as a function of wavelength. The results obtained in Table 2 for optical device D2 also show, as a function of wavelength, increases of 4.55, 4.63, and 4.65 dB at 635 nm, 1310 nm, and 1550 nm, respectively, which means a much lower contrast between different wavelengths than with D1. The other main difference is that the increase in the insertion loss when adding waveguides B and C to D2 is double the increase experienced when adding waveguides B and C to D1. This can be explained by the fact that the waveguides in D2 are thinner than in D1, which leads to a greater perturbation of the waveguide and structure and, hence, of the transmitted signal when new waveguides are added. Finally, the results in Table 3 for D3 show completely different behaviour. The insertion loss after the adhesion of two PDMS waveguides increased by 0.15 dB at 635 nm and 0.33 dB at 1550 nm or decreased by 0.35 dB at 1310 nm. The explanation for the small increase in the insertion loss of D3 compared to the results obtained with waveguides of the same diameter in D2 is that in D3 air bubbles were suppressed, which leads to a more uniform and material with less scattering. Consequently, the light is transmitted in a more directive way, without being affected by the presence of additional waveguides attached to waveguide A.

However, the better performance of D3 in terms of directive guidance of light through the main PDMS waveguide becomes a drawback when coupling to the rest of the waveguides is analysed. This is shown in Fig. 3c, where coupling to waveguides A, B, and C is shown for the three optical devices at the second telecommunication window, 1310 nm. It is observed that the worst case is a waveguide without trapped air bubbles, where light is more directive, and, consequently, less power is coupled to waveguides B and C

TABLE 4. Insertion losses in the three PDMS waveguides of device D1.

Output	λ=635 nm	λ=1310 nm	λ=1550 nm
A	18.33	17.21	17.64
B	18.57	18.22	19.07
C	21.13	23.08	24.52

(about 10 dB is lost in each waveguide). Conversely, the insertion loss with trapped air bubbles (devices D1 and D2) is not so different due to the higher scattering induced by the bubbles. Moreover, if we compare devices D1 and D2, it is evident that in D1 there is a greater increase in the difference of insertion loss among the different waveguides because, due to the thicker waveguides used in D1, less power is coupled to waveguides B and C compared to optical device D2, where thinner waveguides were used.

More detailed results can be found in Tables 4, 5, and 6, where an analysis at 635, 1310, and 1550 nm is shown for devices D1, D2, and D3, respectively. In Table 4 (tapping optical device D1), the insertion loss in waveguide B and waveguide C is 1.23 and 5.18 dB higher, respectively, on average than in waveguide A for the three wavelengths analysed. In Table 5 (tapping optical device D2), the insertion loss for waveguides B and C is 0.89 and 2.86 higher, respectively, on average than for waveguide A for the three wavelengths analysed. Finally, in Table 6 (tapping optical device D3), the insertion loss in waveguides B and C is 9.8 and 19.3 higher, respectively, on average than in waveguide A for the three wavelengths analysed.

The experimental results demonstrate that more scattering is obtained with D1 and D2 compared to D3 because they present air bubbles. As a result, it is possible to couple more light into waveguides B and C. Regarding the comparison

TABLE 5. Insertion losses in the three PDMS waveguides of device D2.

Output	λ=635 nm	λ=1310 nm	λ=1550 nm
A	15.84	15.12	16.04
B	16.40	15.58	17.68
C	18.90	17.21	19.47

TABLE 6. Insertion losses in the three PDMS waveguides of device D3.

Output	λ=635 nm	λ=1310 nm	λ=1550 nm
A	21.87	14.39	15.84
B	30.22	25.38	25.89
C	39.61	35.04	35.34

of the performance of the structures with air bubbles, using thinner waveguides is better because more light is coupled. In summary, for the performance in terms of balanced coupling, D2 (waveguides with air bubbles and a thickness of 0.5 mm) is better than D1 (waveguides with air bubbles and a thickness of 0.8 mm), and D2 is better than D3 (waveguides without air bubbles and a thickness of 0.5 mm), whereas the opposite is true in terms of power losses of waveguide A when one or more waveguides are added to the optical device. However, it must be highlighted that 20 dBs of additional loss in a waveguide without air bubbles is not practical in terms of preserving an output signal directly from the input without tapping. Therefore, both D1 and D2 optical tapping devices are a better option for this specific application. The insertion loss is higher than the value obtained for an ideal 1 × 3 splitter, which is 4.78 dB according to the equation presented in the introduction section. However, the devices analysed in this work, for the sake of easy handling, presented a length of 1 cm, which is not optimal in terms of insertion losses. By reducing the length of the device, this parameter could be drastically improved. Insertion losses are also important in terms of operating at high frequencies since photodetectors decrease the sensitivity at higher frequencies, i.e., at higher bitrates.

B. THEORETICAL ANALYSIS

To corroborate and better understand the experimental results, some simulations were performed. The air bubbles cause light to scatter, spreading the Gaussian beam. This spread increases continuously as the beam propagates into the PDMS waveguide, leading to an increase in the light coupled to optical fibres at the output end of the tapping devices. The air bubble size was not considered directly in the simulation because of the characteristics of the software used (FIMMPROP). However, the broadening of the Gaussian beam, the main effect of the presence of bubbles in our experiment, was taken into account by increasing the waist of the beam at the output end up to the mode field radius of the fundamental mode supported by the PDMS. According to the guidance conditions, this is the maximum possible value.

Finally, regardless of the type of scattering (determined by the relationship between the size of the air bubbles and the wavelength of the light used for illuminating), the scattered light must satisfy the guidance conditions and hence will be coupled to propagation modes of the waveguide. It is worth noting that the PDMS structure supports a very high number of modes, and under this condition the field profile could be approximated with a Gaussian beam whose radial distribution and power are described by the following expressions [15]:

$$f(x,y) = \exp\left\{-\frac{r^2}{w_0^2}\right\} \tag{1}$$

$$P_{in} = \frac{\pi}{2}\left(\frac{\varepsilon_0}{\mu_0}\right)^{1/2} n_{co}\rho^2 \tag{2}$$

where $r^2 = x^2 + y^2$ is the radial coordinate, and n_{co} and w_0 are the refractive index of the core and the modal field radius of the optical fibre, respectively. Because of the dimensions of the devices, the setup operates far from the diffraction limit. Therefore, the Gaussian beam spreads as it propagates into the tapping device. At position z, on the end face of the device, the profile of the Gaussian beam could be expressed as the following [16]:

$$f(x,y) = \exp\left\{-\frac{x^2+y^2}{w(z)^2}\right\} \tag{3}$$

where $w(z) = w_0\sqrt{1+\left(\frac{z}{z_0}\right)^2}$ is the waist of the Gaussian beam at position z and $z_0 = \frac{\pi w_0^2 n_{PDMS}}{M\lambda_0}$. M is a parameter that relates the radius of the Gaussian beam to the numerical aperture of the multimode fibre and can be written in an approximated form as $M = NA\pi w_0/2\lambda_0$.

Under these approximations and considering that the light will be mainly coupled from the input field to the fundamental mode of the output multimode fibres, we used FIMMPROP (FIMMWAVE) to estimate the optical power coupling between the Gaussian beam and the optical fibres at the output of the optical tapping device. The simulation consists of two segments: one for the region of PDMS and the other one for the region that includes both PDMS and the receiving fibre. In both cases, a FIMMWAVE MWG waveguide was used to represent the square section geometry of the structure. The finite difference method (FDM) based mode solver was used to obtain 2 modes (the fundamental mode of the PDMS waveguide and the fundamental mode of the multimode fibre) and the mode profile resolution was nx = 500 ny = 500. The PDMS dimensions were adjusted for fitting the distribution of the fundamental mode of the waveguide to the profile of the Gaussian beam described by expression 3.

A schematic illustration of the simulated structure is shown in Fig. 4a, whereas in Fig. 4b the simulated output segment section is represented, where the receiving fibre is progressively shifted from the region of maximum coupling in order to analyse the power it couples and, hence, the insertion losses (the calculated optical field intensity of the fundamental mode is also presented). Fig. 4c shows the insertion loss as a function of the separation of fibre from the centre of the PDMS waveguide and for different values of the PDMS width. For the sake of simplicity, a horizontal shift is represented, but it must be pointed out that in the simulation a vertical shift was analysed, according to the setup of

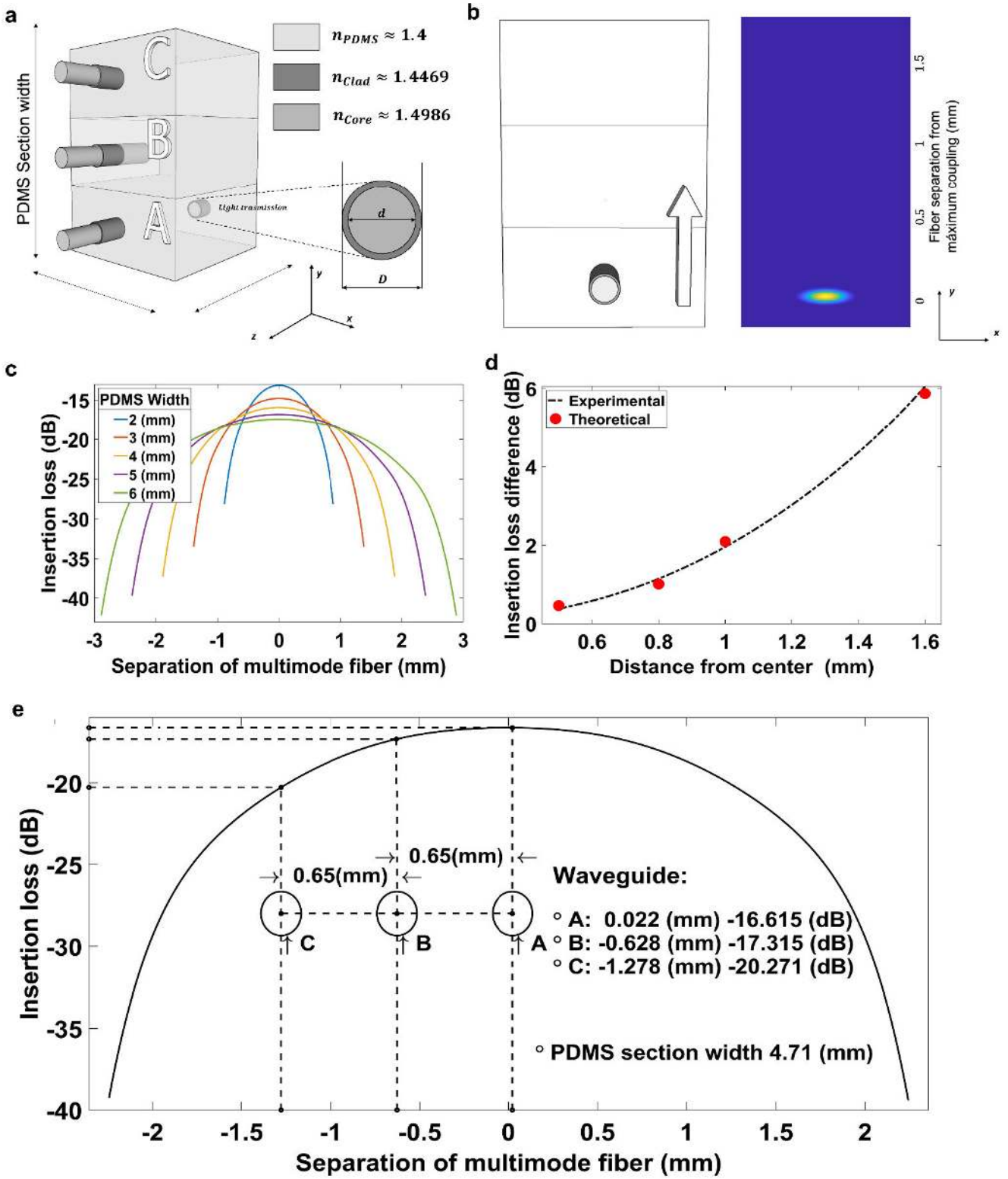

FIGURE 4. Theoretical analysis of the insertion loss. (a) Schematic illustration of the structure analysed with FIMMWAVE. (b) A section representing one of the received fibres that was shifted to analyse the power it couples (the calculated optical field intensity of the fundamental mode is also presented). (c) Insertion loss as a function of the separation of the receiving multimode fibre from the centre of the PDMS waveguide (different widths of the PDMS waveguide were analysed: 2, 3, 4, 5,and 6 mm). (d) Fitting of the PDMS width to match the insertion loss observed in the experimental results (an average PDMS waveguide thickness between D1 and D2 was used). A video showing the evolution of the insertion loss is included in the file Visualisation S2. (e) Insertion loss difference between the fibre at the centre of the PDMS and the fibre shifted from the centre to the outer border. There is an exponential increase in the insertion loss as a function of the separation between the fibres (i.e., the PDMS waveguide thickness). Dotted line: calculated values. Red dots: measured values.

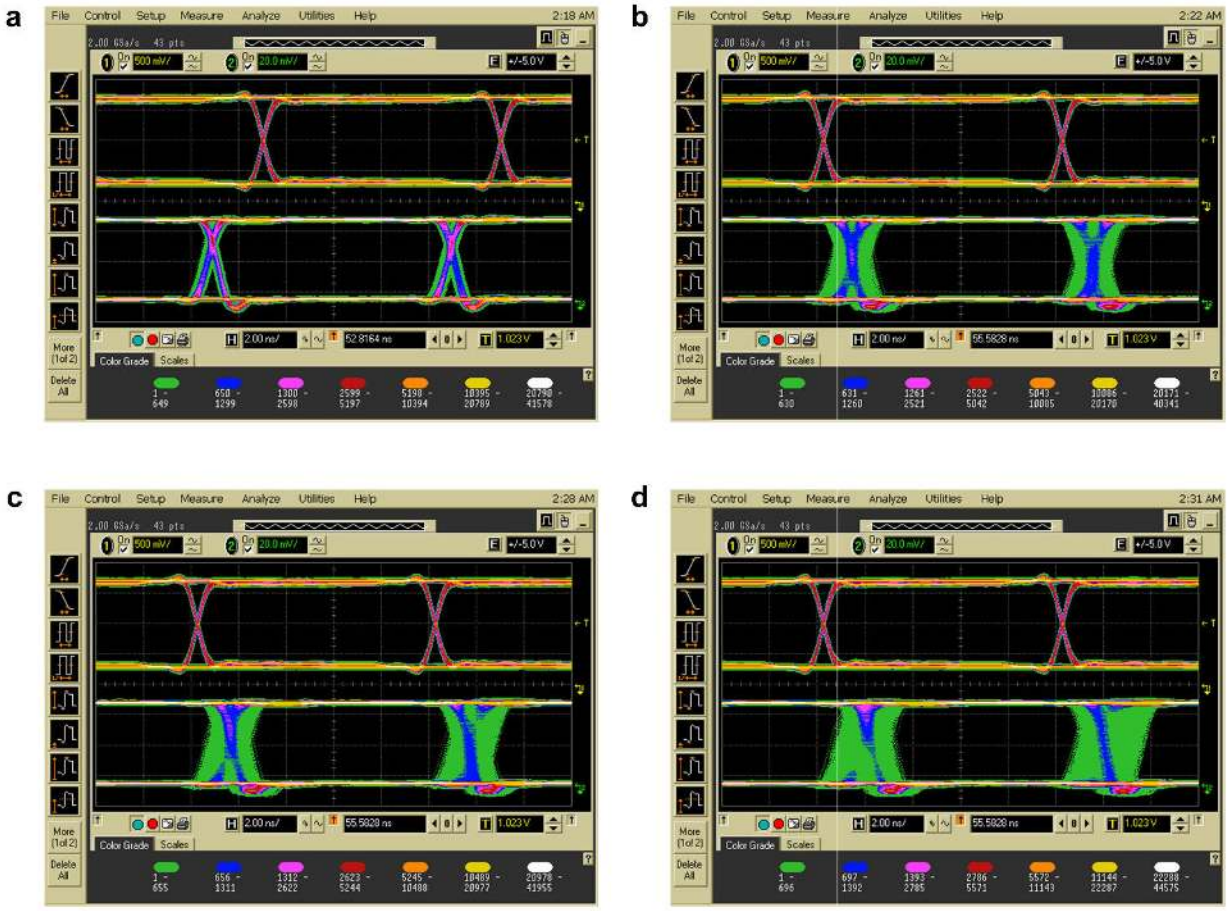

FIGURE 5. Analysis of the performance of the optical tapping device using the setup for communications of Fig. 1b and eye diagrams of the signal transmitted compared to the signal received. (a) Direct transmission through the optical fibre. (b–d) Transmission through waveguides A, B, and C when light is introduced in waveguide A.

Fig. 4a. The horizontal shift in Fig. 4c only aims to simplify the visualisation of the simulation results (see visualisation S2 file). As expected from coupled theory, the insertion loss for a fibre located near the centre of the PDMS is lower compared to a fibre close to the outer edges. This occurs because the width of the optical tapping device is smaller than the waist of the Gaussian beam, and, by the total internal reflection phenomenon, a significant amount of the light will be confined in the optical tapping device. In each simulation, the calculated values of insertion loss were compared with the measured values reported in Fig. 3c in order to determine the PDMS width that fulfils the conditions imposed by the experimental setup.

In Fig. 4d, the variation of the insertion loss with the position of the fibre from the centre of the PDMS is presented for the PDMS width that best fitted the experimental results: 4.71 mm. The insets represent three optical fibres, A, B, and C, located at the following specific positions from the PDMS centre: 0.022 mm, − 0.628 mm, and 1.278 mm, and separated by 0.65 mm. This separation distance is the average of the separations used in the experimental setups of optical devices D1 and D2.

The dependence of the position on the insertion loss difference is shown in Fig. 4e. The dotted black line and the red dots represent the calculated and measured values, respectively. The measured values of insertion loss for 0.5 mm and 1.0 mm were obtained from the D2 optical device, while at the positions of 0.8 mm and 1.6 mm the values were obtained from the D1 optical device. In both cases, a laser source with a wavelength at 1310 nm was used to illuminate the optical tapping device.

C. ANALYSIS OF THE EYE DIAGRAM

After studying the insertion loss of the optical tapping device, a practical test of the performance of the device in optical communications was implemented. The setup (see Fig. 1a) consisted of a pulse generator added to the system with a module to generate patterns for the analysis of eye diagrams. This pulse generator modulates an optical source, and the resulting signal is introduced in the input of the optical device. One of the outputs is connected to the receiver, which, in turn, is connected to an oscilloscope that permits the comparison of the eye diagram of the input and the output signal.

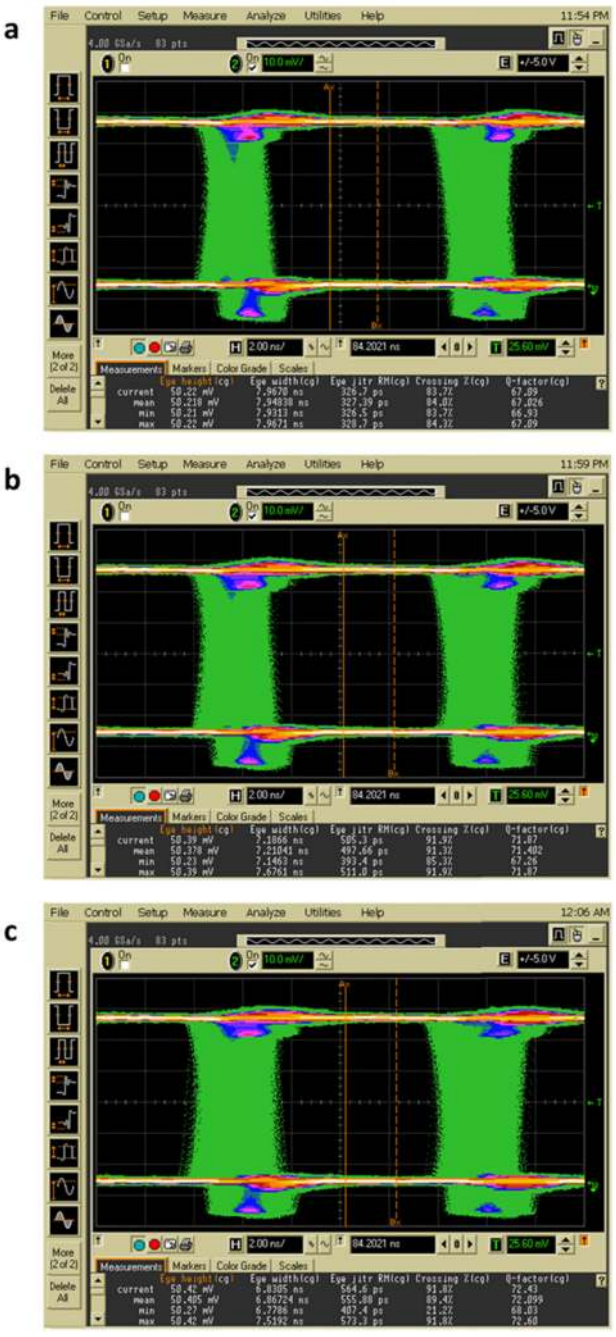

FIGURE 6. Eye diagram of the signal transmitted in the setup of Fig. 1b along with the main parameters. Three cases were studied: (a) transmission through waveguide A, (b) transmission through waveguide B, and (c) transmission through waveguide C.

For this purpose, the D2 device was tested in four cases:

A) direct transmission through an optical fibre, i.e., through the multimode optical fibre used in the setup of Fig. 2 but without passing through the optical device; B) transmission through waveguide A in the optical device; C) transmission through waveguide B in the optical device; and D) transmission through waveguide C in the optical device.

In all cases in Fig. 5, the results are compared with the signal that is being transmitted above in the image of the oscilloscope, while below the signal of the direct transmission through the optical fibre or the transmission through one of the waveguides is presented. In addition, the main parameters of the eye diagram are shown as a reference in Table 7.

TABLE 7. Eye diagram parameters for the three waveguides of device D2.

Eye Diagram Parameters (mean values)	Waveguide A	Waveguide B	Waveguide C
Eye height (mV)	50.218	50.378	50.405
Eye width (ns)	7.94838	7.21041	6.86724
Eye jitter RM (ps)	327.39	497.66	555.88
Crossing (%)	84.0	91.3	89.4
Q-factor	67.026	71.402	72.099

For instance, the insertion losses can be obtained by comparing the eye height of waveguides A, B and C with the eye height for the direct transmission in Fig. 5. With this consideration, 14.34, 14.33, and 14.33 dB were calculated for waveguides A, B, and C, respectively.

These results refer to device D2, whose values were previously analysed in Table 5 at 1310 nm for the laser source. The insertion loss was similar but with the particularity that differences among the waveguides were higher. The reason is attributed to the utilisation of a laser source, whose radiation pattern is more directive than a LED, but it proves that the structure operates both with LED- and laser-based configurations.

Other interesting parameters in Table 7 are the eye width and the jitter, which decrease and increase, respectively, as we move from the PDMS waveguide A, the main waveguide, to waveguides B and C. However, it is possible to observe the eye in all cases, which proves the ability to transmit through the three waveguides of the optical tapping device at the same time. Moreover, the parameters could be improved with a more sensitive receptor and by reducing the length of the PDMS waveguides. More information on the parameters is presented in Fig. 6, where it is also proven that it is possible to operate without the trigger of the transmitted signal.

Fig. 5 and the eye diagram parameters shown in Table 7 demonstrate the possibility of using this optical device to transmit digital baseband signals from one emitter to several receivers at capacities of at least 100 Mbps, opening the path for the design of an optimised device operating at 1 Gbps in residential networking and other data and communications networks.

In the case of optical tapping devices, waveguides similar to D2 (the thinner ones without applying a vacuum process) are the most convenient ones. In this case, the signal is tapped by stacking a new waveguide to the device, which can be dynamically removed when necessary. By introducing different signals from different sections of the input waveguide, we could also use the device as a passive optical combiner/splitter.

IV. CONCLUSION

The implementation of an extremely low cost and dynamic passive optical tapping device was demonstrated, i.e., an

optical device formed by planar waveguides that can be stacked or removed depending on the need of the designer or the user. This dynamic multi-substrate passive and stackable optical tapping device makes it possible to transmit digital signals from the input waveguide to several outputs at the same time, and its good performance for use in data networks has been demonstrated.

This idea was proven with PDMS, which is a flexible material that can easily be adhered or removed. The scattering of light transmitted through a PDMS waveguide was controlled on the basis of the presence of trapped air bubbles inside it. In this sense, two cases were analysed: one without any treatment, where air bubbles are trapped inside the waveguide, and one where the air bubbles are removed from the waveguide with the aid of a vacuum pump. The results were quite different in both cases. With air bubbles, the light scattering was very high, and it was easy to couple light from one waveguide to another. However, there was also an increase in insertion loss in the main waveguide after adhesion of other waveguides. Conversely, without air bubbles, insertion losses in the main waveguide were reduced but coupling to the rest of the waveguides of the stack was low, preventing the possibility of a balanced transmission of light through the different waveguides. Consequently, the design without vacuum was preferred, and this design was analysed with FIMMWAVE, which made it possible to observe an exponential increase in losses as a function of the distance among the waveguides, something that agreed with the experiments.

The effect of the waveguide thickness on the results was also analysed both theoretically and experimentally: a less balanced coupling of light to the outputs of the optical tapping device was obtained with thicker waveguides because there was a higher separation among the waveguides. However, insertion losses were reduced.

All this proves the great versatility of the optical device, whose performance can be controlled with the scattering of light and the waveguide thickness. Moreover, there is still the option to modify the waveguide length. Here, 1 cm long waveguides were used, but other lengths could be explored in further work with the aim of improving the performance of the device, which would permit its use in 1 Gbps networks. Furthermore, here only the more fundamental possibility of introducing a signal by one of the inputs has been explored, but the path is open towards exploring the parallel excitation of several waveguides at the same time, of including an external modulator in the optical tapping device, or of nanocoating the waveguides with metals or metallic oxides towards the excitation of resonances that can be used for sensing or as optical filters, or others that photonic designers may discover on the basis of this novel and simple structure.

REFERENCES

[1] M. Z. Iqbal, H. Fathallah, and N. Belhadj, "Optical fiber tapping: Methods and precautions," in *Proc. 8th Int. Conf. High-Capacity Opt. Netw. Emerg. Technol. (HONET)*, Riyadh, Saudi Arabia, Dec. 2011, pp. 164–168, doi: 10.1109/HONET.2011.6149809.
[2] S. Gorshe, A. R. Raghavan, T. Starr, and S. Galli, *Broadband Access: Wireline and Wireless—Alternatives for Internet Services*, Hoboken, NJ, USA: Wiley, 2014, p. 21.
[3] H. Candong, L. Yong, L. Sheng, and P. Zhixiang, "Integrated 16-way optical divider and preparation method thereof," China Patent 106 291 815 A, Jan. 4, 2017.
[4] L. Wu, K. He, T. Bai, and L. Lin, "Single-mode optical fiber coupling structure of multiple transverse mode laser," China Patent 104 749 715 B, Jul. 1, 2015.
[5] *Tapping of Fibre Networks*, Deloitte, London, U.K., 2017.
[6] U. Eduok, O. Faye, and J. Szpunar, "Recent developments and applications of protective silicone coatings: A review of PDMS functional materials," *Prog. Organic Coatings*, vol. 111, pp. 124–163, Oct. 2017.
[7] P. Abgrall and A.-M. Gué, "Lab-on-chip technologies: Making a microfluidic network and coupling it into a complete microsystem—A review," *J. Micromech. Microeng.*, vol. 17, no. 5, pp. R15–R49, May 2007.
[8] S. Seethapathy and T. Górecki, "Applications of polydimethylsiloxane in analytical chemistry: A review," *Anal. Chim. Acta*, vol. 750, pp. 48–62, Oct. 2012.
[9] Y. Hwang and R. N. Candler, "Non-planar PDMS microfluidic channels and actuators: A review," *Lab Chip*, vol. 17, no. 23, pp. 3948–3959, 2017.
[10] V. Prajzler, M. Neruda, and P. Nekvindová, "Flexible multimode polydimethyl-diphenylsiloxane optical planar waveguides," *J. Mater. Sci., Mater. Electron.*, vol. 29, no. 7, pp. 5878–5884, Apr. 2018.
[11] K. Eyer, K. Root, T. Robinson, and P. S. Dittrich, "A simple low-cost method to enhance luminescence and fluorescence signals in PDMS-based microfluidic devices," *RSC Adv.*, vol. 5, no. 17, pp. 12511–12516, 2015.
[12] M. S. Wróbel, A. P. Popov, A. V. Bykov, V. V. Tuchin, and M. J drzejewska-Szczerska, "Nanoparticle-free tissue-mimicking phantoms with intrinsic scattering," *Biomed. Opt. Exp.*, vol. 7, no. 6, p. 2088, Jun. 2016.
[13] F. Ziegert, M. Koof, and J. Wagner, "A new class of copolymer colloids with tunable, low refractive index for investigations of structure and dynamics in concentrated suspensions," *Colloid Polym. Sci.*, vol. 295, no. 9, pp. 1563–1574, Sep. 2017.
[14] D. Kacik, P. Tatar, and I. Martincek, "Measurement of PDMS refractive index by low-coherence interferometry," in *Proc. ELEKTRO*, Rajecké Teplice, Slovakia, May 2014, pp. 662–665.
[15] A. W. Snyder and J. Love, *Optical Waveguide Theory*. London, U.K.: Chapman & Hall, 1991.
[16] Y. M. Sabry, H. Omran, and D. Khalil, "Intrinsic improvement of diffraction-limited resolution in optical MEMS Fourier-transform spectrometers," in *Proc. 31st Nat. Radio Sci. Conf. (NRSC)*, Cairo, Egypt, Apr. 2014, pp. 326–333, doi: 10.1109/NRSC.2014.6835093.

ISMEL DOMÍNGUEZ received the degree in telecommunications and electronics engineering from the University "Hermanos Saiz Montes de Oca (UPR)," Pinar del Rio, Cuba, in 2009. He is currently pursuing the Ph.D. degree with the Department of Electrical and Electronic Engineering, Public University of Navarra (UPNA). His current research interests include optical fiber sensors and microfluidics.

IGNACIO DEL VILLAR (Member, IEEE) received the M.S. degree in electrical and electronic engineering and the Ph.D. degree, specialty in optical fiber sensors from the Public University of Navarra (UPNA), in 2002 and 2006, respectively. He has been a Reader with the Public University of Navarra, since 2008, an Associate Editor of the *Optics and Laser Technology* journal, since 2012, and *Sensor* journal, since 2017. His research interests include optical fiber sensors and the effect of nanostructured coatings deposited on waveguides, where he has coauthored more than 150 chapter books, journals, and conference papers.

JORGE MONTOYA-CARDONA received the B.S. degree in telecommunications engineering from the Instituto Tecnologico Metropolitano (ITM), Medellín, Colombia. He is currently working as an Assistant Researcher with ITM, supporting the area of modeling of fiber optic devices, where he has coauthored six journals and two conference papers.

OMAR FUENTES received the degree in automatic engineering from the Higher Polytechnic Institute José A. Echeverria (CUJAE), Havana, Cuba, in 1996. He is currently working as an Assistant Professor with the Department of Telecommunication and Electronic Engineering, Pinar del Río University (UPR), Cuba. His current research interests include optical fiber sensors and based on planar waveguide systems.

NELSON D. GÓMEZ-CARDONA received the B.S. degree in physic engineering and the M.Sc. degree in physics from the National University of Colombia, Medellín, Colombia, where he is currently pursuing the Ph.D. degree in physics. He is currently working as an Assistant Professor with the Department of Electronics and Telecommunication, Instituto Tecnologico Metropolitano (ITM), Medellín, where he has founded the Optics, Photonics, and Computer Vision Laboratory. His research interests include computational modeling of specialty optical fibers for applications in sensors and communications, Bragg and long-period fiber gratings in optical fibers, and fiber lasers.

JESUS M. CORRES (Member, IEEE) received the M.S. degree in electrical engineering and the Ph.D. degree from the Public University of Navarra, Pamplona, Spain, in 1996 and 2003, respectively. He is currently working as an Associate Professor with the Department of Electrical and Electronic Engineering (UPNA). He is the author or coauthor of more than 100 publications. His main research interest includes development of fiber optic sensors using nanostructured materials for biomedical, environmental, and safety applications. He serves as an Associate Editor for IEEE Sensor Letters and *Journal of Sensors* (Hindawi).

IGNACIO R. MATIAS (Senior Member, IEEE) received the M.S. degree in electrical and electronic engineering and the Ph.D. degree in optical fiber sensors from the Polytechnic University of Madrid (UPM), Madrid, Spain, in 1992 and 1996, respectively. He became a Lecturer with the Public University of Navarra, Pamplona, Spain, in 1996, where he is currently a Permanent Professor. He has coauthored more than 200 journal and 250 conference papers related to optical fiber sensors and passive optical devices and systems. He was a Co-Founder Editor of IEEE Sensors Journal.